On the Absence of Detectable Carrier Multiplication in a Transient Absorption Study of InAs/CdSe/ZnSe Core/Shell1/Shell2 Quantum Dots

ARTICLE *in* NANO LETTERS · MAY 2008

Impact Factor: 13.59 · DOI: 10.1021/nl080199u · Source: PubMed

NANO LETTERS

2008
Vol. 8, No. 4
1207-1211

On the Absence of Detectable Carrier Multiplication in a Transient Absorption Study of InAs/CdSe/ZnSe Core/Shell1/Shell2 Quantum Dots

Meirav Ben-Lulu,[†] David Mocatta,[†,‡] Mischa Bonn,[§] Uri Banin,[†,‡] and Sanford Ruhman*,[†]

Institute of Chemistry, the Farkas Center for Light Induced Processes, and the Center for Nanoscience and Nanotechnology, The Hebrew University of Jerusalem, Jerusalem 91904, Israel, and FOM Institute for Atomic and Molecular Physics (AMOLF), Kruislaan 407, 1098 SJ Amsterdam, The Netherlands

Received January 21, 2008; Revised Manuscript Received February 22, 2008

ABSTRACT

Tunable femtosecond pump−near IR probe measurements on InAs/CdSe/ZnSe core/shell1/shell2 nanocrystal quantum dots were conducted to quantify spontaneous carrier multiplication previously reported in this system. Experimental conditions were chosen to eliminate the need for determining absolute wavelength dependent cross sections of the nanocrystals and allow direct comparison of band edge absorption bleach kinetics for different excitation energies up to 3.7 times the band gap. Results for two sample sizes show no signs of carrier multiplication within that range. This result is discussed in light of reports describing occurrence of this novel phenomenon in quantum dots based on this as well as numerous other semiconductor materials.

Efficient carrier multiplication (CM) in semiconductor nanocrystal quantum dots (QD) has been reported for a slew of different materials including CdSe, PbS, PbSe, InAs, PbTe, and Si.[1–10] In this process, absorption of a single energetic photon leads to generation of two or more electron–hole pairs. The interest in this phenomenon stems from the fundamental importance of understanding the underlying mechanism and in particular the role quantum confinement plays in its realization. It has also generated interest due to its practical ramifications.[11] CM in nanocrystals potentially overcomes shortcomings of bulk semiconductor photovoltaic materials that provide at most a single band gap of electric energy regardless of the photon wavelength. CM was proposed as a possible mechanism to allow more complete conversion of photon energy into electric potential for a broad spectrum of wavelengths through the generation of multiple electron–hole pairs.[6] This would also reduce detrimental heat generation that accompanies incomplete conversion. Here we report a protocol for probing CM in QDs using femtosecond transient absorption (TA) spectroscopy. Applying the method to InAs/CdSe/ZnSe core/shell1/shell2 (CSS) QDs has revealed no evidence for CM in this system up to 3.8 times the gap energy.

Demonstration of CM has relied on the disparity of single and multiple exciton decay kinetics in semiconductor QD's.[12–14] Well passivated semiconductor nanocrystals, and particularly semiconductor core/shell systems, can reach emission quantum efficiencies (QE) of their single exciton states near unity, with radiative lifetimes of tens to hundreds of nanoseconds. In contrast, multiple excitons decay much more rapidly to long-lived monoexciton states via Auger recombination,[15,16] which is essentially the inverse of carrier multiplication. Quantum confinement enhances the rate of this process, resulting in relaxation from multi- to monoexcitons within a few tens of picoseconds. This separation of timescales allows estimation of the initial multiple vs single exciton occupation numbers by monitoring excited-state decay kinetics, either by recording the absorption bleach kinetics at the band edge,[1–10] or by directly time-resolving photoluminescence.[17] An earlier report concerning CM in samples equivalent to those studied here including work by some of the authors[7] was based primarily on THz probing of the intrinsic hole absorption. The CM assignment reported in that publication is refuted here. The results retracted are

* Corresponding author. E-mail: sandy@fh.huji.ac.il.
[†] Institute of Chemistry and the Farkas Center for Light Induced Processes, The Hebrew University.
[‡] Center for Nanoscience and Nanotechnology, The Hebrew University of Jerusalem.
[§] FOM Institute for Atomic and Molecular Physics.

10.1021/nl080199u CCC: $40.75
Published on Web 03/15/2008

most likely due to an incorrect determination of absorption cross sections (for details, see correction[18]).

Multiple exciton states are however generated not only through CM but also by consecutive multiphoton absorption, posing a significant obstacle in the path of quantifying CM from TA data. Above band gap irradiation necessarily leads to single as well as multiple exciton states with probabilities that follow Poisson statistics:[2,15]

$$P_N = \frac{e^{-\eta}\eta^N}{N!} \quad ; \quad \eta \equiv J\sigma_P \tag{1}$$

J is the photon flux, σ_P is the absorption cross section at the pump wavelength, and N the number of absorbed photons. η is the average number of photons absorbed per QD. Accordingly, one can limit the relative probability for multiphoton absorption by reducing the pump fluence, but it cannot be completely eliminated and its control comes at the cost of reduced signal levels. This is particularly enhanced by the steep rise in absorption cross section with photon energy, resulting for example in $(\sigma_{3BG}/\sigma_{BG}) \geq 20$, where σ_{BG} and σ_{3BG} are the absorption cross sections for photon energies equal to the band gap and three times that, respectively. This vast difference in absorption cross sections has two consequences: first, to directly excite equal distributions of exciton states for different pump wavelengths one must scale the excitation photon flux J so as to conserve η. This can lead to vanishingly small fluences as σ rises rapidly at shorter pump wavelengths. A second consequence is that unless one employs samples that are optically thick or thin at all the different pump wavelengths studied, conserving constant η alone will not lead to equal distributions of exciton occupation numbers. This is a consequence of the exponential depletion of the pump beam as it traverses the sample, an effect that is highly wavelength dependent.

Let us describe this quantitatively. In optically thick samples, the photon density per unit area varies as the laser beam traverses the cell, causing η to change from η_0 before to η_∞ after the cell. To estimate ρ_N, the density per unit area of QDs excited with N photons, we use eq 1 above, $P_A = 1 - e^{-\eta}$, the probability of absorbing at least 1 photon, and $\eta_A = \eta/(1 - e^{-\eta})$, the average number of photons per *absorbing* QD to derive eq 2:

$$\rho_N = \int_{\eta_0}^{\eta_\infty} \frac{e^{-\eta}(\eta)^{(N-1)}}{N!}\frac{d\eta}{\sigma} \tag{2}$$

which quantifies the influence of the sample OD on the exciton occupation numbers. The states coupled by the band gap transition in InAs are 2-fold degenerate, and therefore relaxed monoexcitons are transparent at the band edge, while relaxed multiexcitons exhibit gain that is nearly equivalent to the ground-state absorption. Accordingly, our measurements bunch photoexcited crystals in 2 groups: those that absorb a single photon, and those that absorb two or more. Using the expressions above, we can calculate the density per unit area of QDs which have absorbed at all, and the density of all multiphoton absorbers respectively as $\rho_{>0}$ and $\rho_{>1}$ and from them, expressions for the immediate band gap absorption bleach $\Delta\alpha_{INST}$ and its residual after Auger recombination of multiexcitons $\Delta\alpha_{SINGLE}$:

$$\rho_{>0} = \int_{\eta_0}^{\eta_\infty} \frac{1 - e^{-\eta}}{\eta}\frac{d\eta}{\sigma} \quad ; \quad \rho_{>1} = \int_{\eta_0}^{\eta_\infty} \frac{1 - e^{-\eta} - \eta e^{-\eta}}{\eta}\frac{d\eta}{\sigma} \tag{3}$$

$$\Delta\alpha_{INST} \cong (\rho_{>0} + \rho_{>1})\sigma_{BG} \quad ; \quad \Delta\alpha_{SINGLE} \cong \rho_{>0}\sigma_{BG}$$

Decay of monoexcitons that takes place during Auger recombination is ignored here.

According to eqs 1−3, a single pump–probe measurement would suffice to determine if spontaneous CM is taking place and to estimate its efficiency. That is, if one is given the absorption cross section, and if bleach components due to multiple and single exciton states are both separable and perfectly linear with number density. But these do not hold perfectly. Cross sections are not easily obtained with significant precision, and the excited-state decays that are modeled as single exponentials are not perfectly described as such as demonstrated in the online supporting information filed with this report showing biexponential emission kinetics in these samples (Figure S4, Supporting Information, ref 20). In addition, band edge bleach spectra are influenced by stark shifting of the remaining transitions.[16] Comparing pump–probe experiments with simultaneous conservation of η and of sample OD at a variety of pump wavelengths is a method of identifying the presence of CM, which circumvents these restrictions. This requires preparation of sample solutions with different concentrations for each pump wavelength, and comparison of experiments at the different λ_{PUMP} using J_0 that are scaled inversely with σ_P, thus ensuring that all density ratios (ρ_{N^*}/ρ_N) are the same regardless of N and N^* (as long as CM is absent). With this approach, it is not necessary to determine absolute cross sections but only to determine the ratio of σ_P for any pair of excitation wavelengths, a measure trivially derived from the linear absorption spectrum. The only assumptions are: (1) that sufficiently above bandgap the cross section is impervious to existing excitations and (2) that multiexciton decay can be kinetically distinguished from that of monoexcitons. Using these conditions, any excess in $(\Delta\alpha_{INST}/\Delta\alpha_{SINGLE})$ or even a significant difference in decay kinetics observed in matching experiments using $h\nu > 2BG$ can serve to demonstrate CM without recourse to additional analysis. This approach has been adopted in our experiments.

The samples studied consisted of InAs/CdSe/ZnSe core–shell−shell (CSS) QDs prepared as previously described.[19] The CSS configuration was chosen because of the stability afforded by the double shell passivation. Two sizes of CSS QDs were investigated. Sample A was prepared from InAs QDs, with a mean diameter of 5.9 nm, onto which one monolayer of CdSe buffer followed by four monolayers of ZnSe were grown. Similarly, sample B was prepared from InAs QDs with a mean diameter of 4.9 nm, onto which one monolayer of CdSe buffer and four monolayers of ZnSe were grown. The final diameters of sample A and B were 6.7 and 5.7 nm, respectively (TEM images and histograms of QD diameters are presented in Figures S1 and S2, Supporting Information[20]). Figure S3 (Supporting Information) shows the absorbance and emission spectra of both samples. Fluorescence lifetime studies were also conducted, showing significantly increased $1/e$ decay times for the CSS QDs

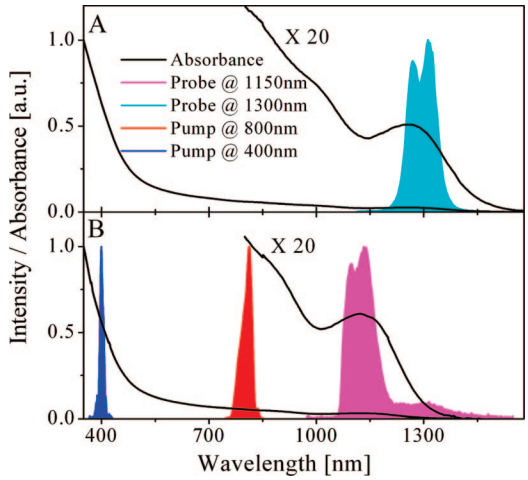

Figure 1. Absorption spectra of (A) 0.95 eV and (B) 1.1 eV band gap CSS samples. Pump and probe intensity spectra used in our measurements are included for comparison.

compared to the respective cores, reflecting the improved surface passivation (Figure S4, Supporting Information).

The laser system consisted of a homemade multipass amplified titanium sapphire laser producing 0.5 mJ, 30 fs pulses at 1 kHz, centered at 790 nm.[21] Excitation pulses at 400 nm were generated by doubling the amplifier fundamental in 0.1 mm of BBO and those at 350 nm by quadrupling the signal output from a parametric amplifier (TOPAS, light conversion). Probe pulses were generated by supercontinuum genearation in 1 mm of N-SF6 glass with part of the amplifier fundamental. Probe pulses at 1.3 μm were isolated by interference filtering (Spectrogon) and at 1.15 μm by a long pass cutoff at 1.1 μm with controlled fluence in the continuum generation stage (see Figure 1 for spectra of laser pulses and sample absorption). A ratio above 2 was maintained between the diameters of pump and probe beams in the sample to ensure we are probing a region of nearly constant photon flux. Probe and reference were recorded on amplified germanium photodiodes (New Focus) using lock-in detection (SR510) before digitization.

Pump–probe data for 0.95 and 1.1 eV band gap QDs (sample A and B, respectively) are depicted in Figure 2. Panels A and B exhibit 800 nm pump−NIR probe results extending to a delay of 650 ps for optically thin samples ($OD_{800nm}^{0.95eV} = 0.23$; $OD_{800nm}^{1.1eV} = 0.11$). At low fluences, the bleach amplitude increases linearly with fluence and exhibits a slow decay extending far beyond our range of delay variation. As the fluence is increased, a stage of rapid bleach decay assigned to Auger recombination is observed for both samples together with a deviation from linear growth in the residual bleach that follows. Finally, at very high fluences, the Auger recombination amplitude nearly equals the monoexciton bleach that follows and further increase of pump fluence leaves the signal nearly intact. These trends are expected because the measurement is ideally only sensitive to the presence of up to two excitons, and once nearly all QDs absorb ≥ 1 photons, the signal will be immune to denser excitation (up to a limit). Also, as expected, the time scale for Auger recombination is shorter for the smaller sample due to enhanced confinement.

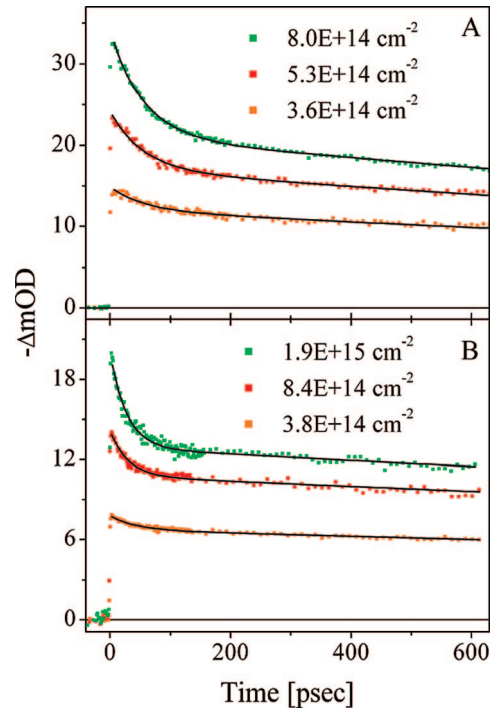

Figure 2. Dependence of TA signals on 800 nm pump photon flux in optically thin (A) 0.95 eV and (B) 1.1 eV band gap CSS samples.

Mindful of the limitations of monoexponential modeling of both decay phases, the ($\rho_{>1}/\rho_{>0}$) ratio was quantified by fitting the data of panel A and B, producing the amplitudes and decay times tabulated in Table 1. The only decay time that is determined with significant precision is that of Auger recombination, which is best fit to 53 and 28 ps for the two samples, respectively. This reduction in time scale is consistent with reports on biexciton decay in InAs and other QDs.[7,16,22] Numerical simulation of ($\rho_{>1}/\rho_{>0}$) at the various pump fluences was conducted using eq 3, and a fitting procedure leads to estimated σ_{800} of 2.0×10^{-15} and 1.2×10^{-15} cm^2 for the 0.95 and 1.1 eV band gap crystals, respectively. Values were independently deduced from the variation of monoexciton bleach amplitudes with fluence, and the values of σ_{800} obtained from both methods match within error. The resulting cross sections are about 40% smaller than values predicted from the E_{BG} and the functional dependence of σ on the QD radii presented in Figure 2 of ref 23.

A comparison of 800 and 400 nm excitation (pump–probe) results for the same QDs (containing 1.7 and 3.3 times E_{BG} for the large QDs and 2.9 and 1.5 for the smaller sample, respectively) are presented in Figures 3 and 4. In both cases, the samples were of OD = 1.2 *at the pump wavelength*, leading to a 5% pump transmission at λ_{PUMP}. For this comparison, optically thick samples were chosen so as to maximize the signal amplitudes, which are reduced by more than an order of magnitude going from 800 to 400 nm pump due to the dilution factor required to conserve σ. The *Y* axes have been scaled by the photon flux ratio, and remarkably, a perfect agreement at all delays is obtained for both excitation wavelengths. In particular, no excess in bleach is

Table 1. Results of Biexponential Fitting of the Data in Figure 2[a]

fluence [photons/cm^2]	η_0 (at the front of the cell)	biexciton lifetimes [ps]	experimental $\Delta\alpha_{INST}/\Delta\alpha_{SINGLE}$	calculated $\Delta\alpha_{INST}/\Delta\alpha_{SINGLE}$
Sample A - 0.95 eV (monoexciton $\tau = 3$ ns; $\sigma_{800} = 2.0 \times 10^{-15} \pm 0.9 \times 10^{-15}$ cm^2)				
3.6×10^{14}	0.5	53 ± 5	1.24	1.3
5.3×10^{14}	0.8	54 ± 2	1.42	1.4
8.0×10^{14}	1.2	53 ± 1	1.62	1.5
Sample B - 1.1 eV (monoexciton $\tau = 5.2$ ns; $\sigma_{800} = 1.2 \times 10^{-15} \pm 0.6 \times 10^{-15}$ cm^2)				
3.8×10^{14}	0.3	28 ± 14	1.16	1.2
8.4×10^{14}	0.7	29 ± 1	1.32	1.3
1.9×10^{15}	1.7	27 ± 1	1.56	1.6

[a] The last column presents calculated amplitude ratios of total to single excitons derived from experimental cross sections.

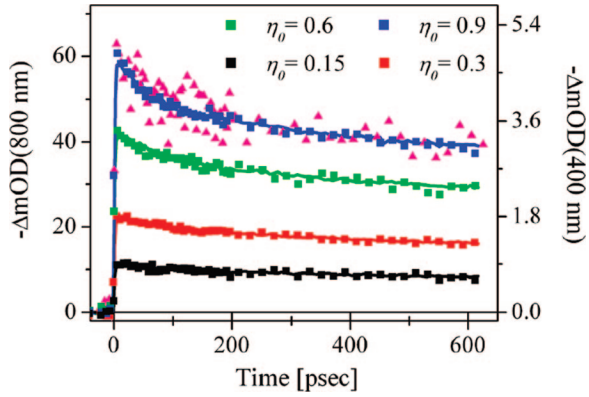

Figure 3. Comparison of band-edge bleach decays following 400 nm (squares), 800 nm (solid lines), and 350 nm (pink triangles) excitation for 0.95 eV band gap CSSs. All experiments were conducted on samples with OD 1.2 at the pump wavelength. Photon flux is given in units of inverse cross sections at the pump wavelength, coined η_0. Notice different Y scales for 800 and 400 nm data. See text for details.

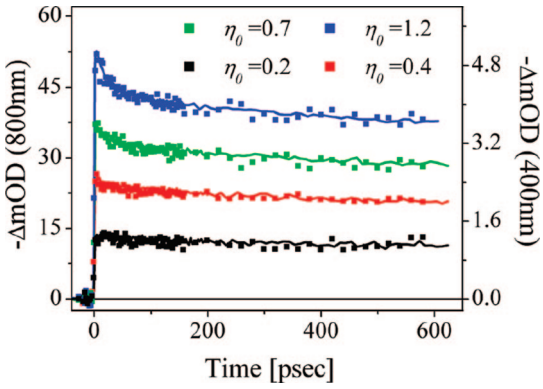

Figure 4. As in Figure 3, for 1.1 eV band gap CSSs.

observed at early times for 400 nm excitation relative to that obtained with 800 nm pump pulses. Also, no rapid phase of bleach decay is apparent for the lowest 400 nm excitation fluence. All of these findings are consistent with total absence of CM up to photon energies of 3.25 E_{BG}. Finally, even when exciting the larger crystals with photons containing 3.54 eV of energy, 3.8 times the band gap (Figure 3, pink triangles), no difference other than the scaling of signal amplitude is observed, as demonstrated in Figure 3 along with matching 800 and 400 nm scans. It is important to point out that in all previous reports on InAs,[7,8] the threshold for appearance of CM was close to twice the band gap, which we have exceeded here considerably for both samples.

One publication has reported the absence of carrier multiplication in CdSe and CdTe nanocrystals based on photoluminescence lifetime studies[24] in contrast to extensive CM found in earlier TA experiments on the CdSe and CdTe systems. In all other semiconductor QDs, significant CM was found using TA methods once excitation wavelengths were tuned sufficiently above the band gap.[1–9] In view of this unique finding, it is appropriate to discuss its relevance to other semiconductor systems. Because of intrinsic inequalities in sample structure, the only report in the literature, part of whose conclusions are refuted here, is that recently presented by some of the authors[7] conducted on equivalent samples and based on THz probing (see above). The only other report on InAs[8] was conducted on InAs−CdSe core–shells, which differ both in the thickness and in the number of shells. Theories promoted for explaining CM in QDs suggest that its efficiency depends on high spatial overlap of mono- and multiexciton states high above the band gap.[2,25,26] This could be affected by the presence of a significant shell layer that is energetically permeable to high energy monoexcitons but less so to biexcitonic states of equal total energy. Therefore, only repeating the described experimental protocol on other samples that differ from that studied here will reveal if our findings carry over to other semiconductor systems or for that matter to other InAs core−shell architectures.

Finally, we pause to compare the methodology described above with that used by others in the analysis of TA data pertaining to the CM phenomenon. That most elaborately described was published by Nozik and co-workers,[10,27] including a detailed account of the difficulties posed by the disparity of cross sections. Their analysis is based on fitting a measure they have coined R_{pop}, which is equivalent to our $(\rho_{>1}/\rho_{>0})$, to an analytical function that is equivalent to our eq 3. This is a systematic way of extrapolating to zero fluence in order to demonstrate that one has reached excitation fluxes that are indicative of that regime. The only difficulty with this approach is that it is based on a number of unnecessary assumptions. The linearity of band edge bleach with exciton number is one, adherence to which depends on the precise probe spectrum.[16] Another is the kinetic separability of mono- and multiexciton signatures assuming exponential decay kinetics for both. Furthermore, its implementation hinges on the collection of high-quality bleach kinetics at low excitation fluences that approach $\rho_{>1} \simeq 0$ even at short excitation wavelengths.

In contrast, the method we have opted for here allows direct comparison of data sets obtained at different excitation energies directly, even when a non-negligible portion of the excited QDs have absorbed more than a single photon, and for cases where the prompt bleach is neither perfectly linear with η nor trivially separable into the said components. To use this method not only requires no absolute absorption cross sections but does not even require their determination from the exciton decays. As stated above, any one of the matched experiments compared in Figures 3 or 4 would suffice to demonstrate that no CM is taking place in this sample at the pertinent short wavelength. Quantification of CM in samples where it *is* detected is another matter, requiring analysis based on approximations such as those used in previous studies.[28] We have, for completeness, included analyses in that spirit for estimating σ, and the inherent assumptions appear to hold reasonably well in the present context. Despite the care we have taken to present a simpler and more general method for testing the existence of CM, similar conclusions concerning its absence in these samples would have been reached on the basis of the fitting procedure described above as well. Thus while our approach requires less uncertain input, in itself it does not explain the discrepancies in the conclusions. Explaining these will accordingly require further study of this intriguing process.

Acknowledgment. This work was supported by the James Frank program for light−matter interactions. The Farkas Center is supported by the Minerva Gesellschaft, GmbH, Munich, Germany. D.M. acknowledges support from the Centre for Scientific Absorption, the Ministry of Absorption, the state of Israel.

Supporting Information Available: Additional characteristics of the samples studied. This material is available free of charge via the Internet at http://pubs.acs.org.

References

(1) Schaller, R. D.; Klimov, V. I. *Phys. Rev. Lett.* **2004**, *92*, 186601.
(2) Ellingson, R.; Beard, M. C.; Johnson, J. C.; Yu, P.; Micic, O. I.; Nozik, A. J.; Shabaev, A.; Efros, A. L. *Nano Lett.* **2005**, *5*, 865.
(3) Schaller, R. D.; Petruska, M. A.; Klimov, V. I. *Appl. Phys. Lett.* **2005**, *87*, 253102.
(4) Schaller, R. D.; Agranovich, V. M.; Klimov, V. I. *Nat. Phys.* **2005**, *1*, 189.
(5) Klimov, V. I. *J. Phys. Chem. B* **2006**, *110*, 16827.
(6) Schaller, R. D.; Sykora, M.; Pietryga, J. M.; Klimov, V. I. *Nano Lett.* **2006**, *6* (3), 424.
(7) Pijpers, J. J. H.; Hendry, E.; Milder, M. T. W.; Fanciulli, R.; Savolainen, J.; Herek, J. L.; Vanmaekelbergh, D.; Ruhman, S.; Mocatta, D.; Oron, D.; Aharoni, A.; Banin, U.; Bonn, M. *J. Phys. Chem C* **2007**, *111*, 4146.
(8) Schaller, R. D.; Pietryga, J. M.; Klimov, V. I. *Nano Lett.* **2007**, *7* (11), 3469.
(9) Murphy, J. E.; Beard, M. C.; Norman, A. G.; Ahrenkiel, S. P.; Johnson, J. C.; Yu, P.; Mićić, O. I.; Ellingson, R. J.; Nozik, A. J. *J. Am. Chem. Soc.* **2006**, *128*, 3241.
(10) Beard, M. C.; Knutsen, K. P.; Yu, P.; Luther, J. M.; Song, Q.; Metzger, W. K.; Ellingson, R. J.; Nozik, A. J *Nano Lett.* **2007**, *7* (8), 2506.
(11) Nozik, A. J. *Inorg. Chem.* **2005**, *44*, 6893.
(12) Guyot-Sionnest, P.; Shim, M.; Matranga, C.; Hines, M. *Phys. Rev. B* **1999**, *60*, 2181.
(13) Klimov, V. I.; McBranch, D. W. *Phys. Rev. Lett.* **1998**, *80*, 4028.
(14) Santori, C.; Solomon, G. S.; Pelton, M.; Yamamoto, Y. *Phys. Rev. B* **2002**, *65*, 073310.
(15) Klimov, V. I.; Mikhailovsky, A. A.; McBranch, D. W.; Leatherdale, C. A.; Bawendi, M. G. *Science* **2000**, *287*, 1011.
(16) Klimov, V. I. *J. Phys. Chem B* **2000**, *104*, 6112.
(17) Schaller, R. D.; Sykora, M.; Jeong, S.; Klimov, V. I. *J. Phys. Chem. B* **2006**, *110*, 25332.
(18) Pijpers, J. J. H. et al., in press.
(19) Aharoni, A.; Mokari, T.; Popov, I.; Banin, U. *J. Am. Chem. Soc.* **2006**, *128*, 257.
(20) See Supporting Information for this article.
(21) Kahan, A.; Nahmias, O.; Friedman, N.; Sheves, M.; Ruhman, S. *J. Am. Chem. Soc.* **2007**, *129*, 537.
(22) Achermann, M.; Hollingsworth, J. A.; Klimov, V. I. *Phys. Rev. B* **2003**, *68*, 245302.
(23) Yu, P.; Beard, M. C.; Ellingson, R. J.; Ferrere, S.; Curtis, C.; Drexler, J.; Luiszer, F.; Nozik, A. J. *J. Phys. Chem. B* **2005**, *109*, 7084.
(24) Nair, G.; Bawendi, M. G. *Phys. Rev. B* **2007**, *76*, 081304.
(25) Shabaev, A.; Efros, Al. L.; Nozik, A. J. *Nano Lett.* **2006**, *6* (12), 2856.
(26) Franceshetti, A.; An, J. M.; Zunger, A. *Nano Lett.* **2006**, *6* (10), 2191.
(27) Luther, J. M.; Beard, M. C.; Song, Q.; Law, M.; Ellingson, R. J.; Nozik, A. J. *Nano Lett.* **2007**, *7* (6), 1779.
(28) Supporting information of ref 2.

NL080199U